

# **Supplementary Materials**

## **One-pot process: microwave-assisted keratin extraction and direct electrospinning to obtain keratin-based bioplastic**

**Elena Pulidori <sup>1</sup>, Simone Micalizzi <sup>2</sup>, Emilia Bramanti <sup>3</sup>, Luca Bernazzani <sup>1</sup>, Celia Duce <sup>1,\*</sup>, Carmelo De Maria <sup>2,\*</sup>, Francesca Montemurro <sup>2</sup>, Chiara Pelosi <sup>1</sup>, Aurora De Acutis <sup>2</sup>, Giovanni Vozzi <sup>2</sup>, Maria Rosaria Tinè <sup>1</sup>**

<sup>1</sup> Department of Chemistry and Industrial Chemistry, University of Pisa, Via G. Moruzzi 13, 56124 Pisa, Italy; elena.pulidori@unipi.it, luca.bernazzani@unipi.it, chiara.pelosi92@gmail.com, mariarosaria.tine@unipi.it

<sup>2</sup> Research Center E. Piaggio and Department of Information Engineering, University of Pisa, Largo L. Lazzarino 1, 56126 Pisa, Italy; simone.micalizzi@phd.unipi.it, Francesca.montemurro@unipi.it, a.deacutis@studenti.unipi.it, giovanni.vozzi@unipi.it

<sup>3</sup> Institute of Chemistry of Organometallic Compounds, National Research Council, via G. Moruzzi 1, 56124 Pisa, Italy; emilia.bramanti@pi.iccom.cnr.it

\* Correspondence: C.D. celia.duce@unipi.it; Tel.: 050 2219311; C.D.M carmelo.demaria@unipi.it; Tel. 050 2217073

## **TABLE OF THE CONTENTS:**

### **1. CHARACTERIZATION OF KERATIN EXTRACT**

1.1. Evaluation of amino acids content (Table S1)

1.2. SDS-PAGE of TSK fractions (Figure S1)

### **2. CHARACTERIZATION OF KERATIN-BASED MATERIAL**

2.1. Uniaxial tensile test (Figure S2 and S3)

2.2. Water permeability (Figure S4 and S5)

2.3. SEM images (Figure S6)

2.4. TG curves (Figure S7)

2.5. DSC curves (Figure S8)

2.6. ATR-FTIR spectra (Figure S9)

# 1. CHARACTERIZATION OF KERATIN EXTRACT

## 1.1. Evaluation of amino acids content:

**Table S1.** Amino acids identify and quantify in the keratin extracts.

Amino acids	mg in the keratin extract								
	2h MAE	2h MAE	5h MAE	5h MAE	2h CH	2h CH	5h CH	5h CH	
Ser*	/	/	/	/	/	/	/	/	/
OH-pro*	/	/	/	/	/	/	/	/	/
Pro	84.62	115.13	104.77	132.40	147.51	161.16	207.23	203.64	
Val	51.50	46.17	80.97	58.60	37.73	53.27	71.03	84.35	
Met	<LOD**	<LOD							
Tyr	0.15	0.16	0.31	0.33	0.21	0.18	0.41	0.42	
Leu	<LOD	<LOD	<LOD	<LOD	<LOD	<LOD	<LOD	<LOD	
Phe	<LOD	<LOD	<LOD	<LOD	<LOD	<LOD	<LOD	<LOD	
Sum	136.27	161.46	186.05	191.33	185.45	214.61	278.68	288.41	
Extraction volume (mL)	200	200	200	200	250	250	250	250	
<b>mg/mL</b>	<b>0.68</b>	<b>0.81</b>	<b>0.93</b>	<b>0.96</b>	<b>0.74</b>	<b>0.46</b>	<b>1.11</b>	<b>1.15</b>	

\*Serine and hydroxyproline are not detectable because they coelute with acetic acid.

\*\*LOD: Limit of detection of Pro= 0.069, Val= 0.069, Met= 0.075, Tyr=0.004, Leu=0.774, Phe= 0.020 mg/mL.

**1.2. SDS-PAGE of TSK fractions:**

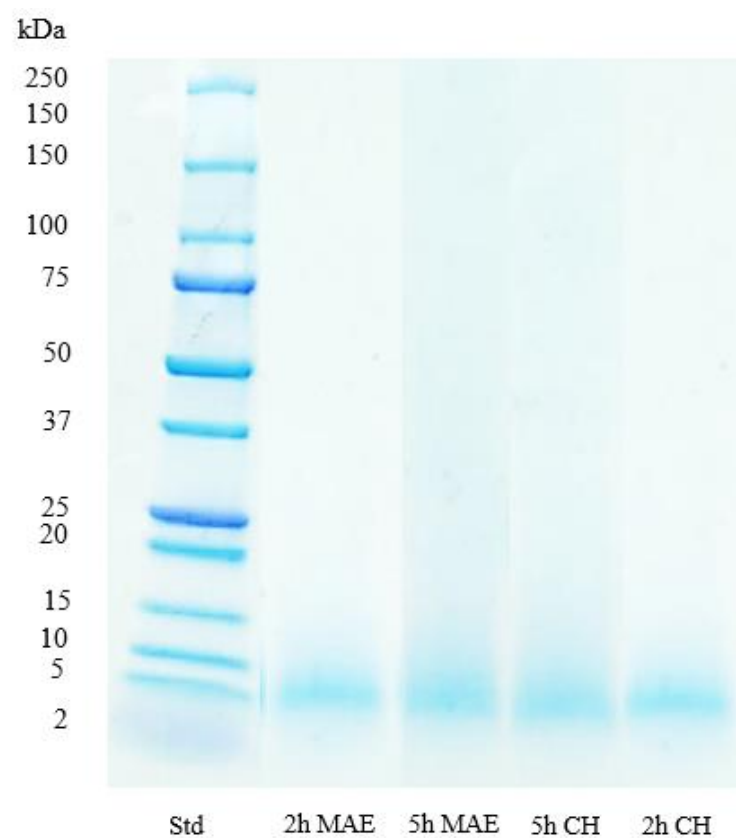


**Figure S1.** SDS-PAGE of standard proteins (Std) and TSK obtained after 2 and 5 h extraction by MAE and CH process.

## 2. CHARACTERIZATION OF KERATIN-BASED MATERIAL

### 2.1. Uniaxial tensile test

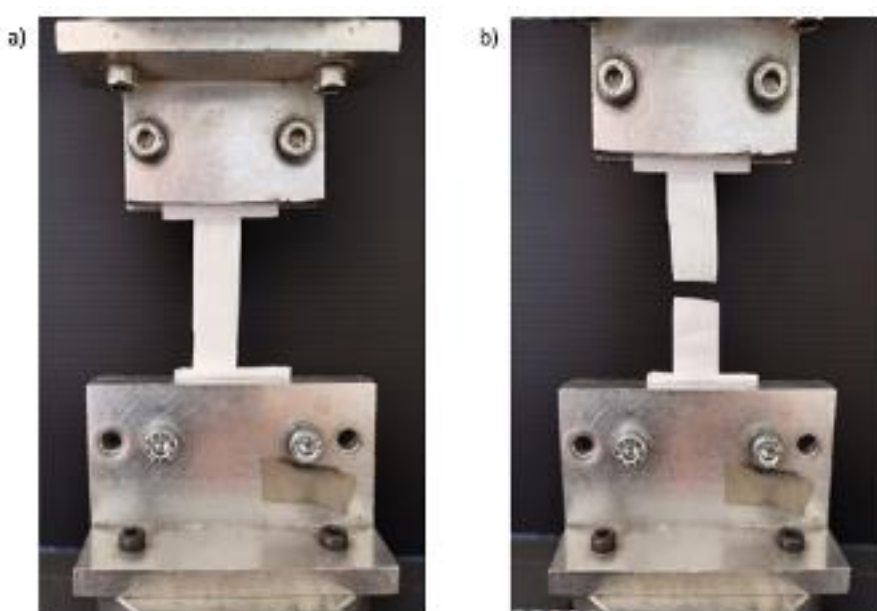


**Figure S2.** Uniaxial tensile test setup for a keratin-based bioplastic specimen before (a) and after (b) failure.

Figure Description:

Setup for the tensile test of the electrospun keratin-based bioplastics. The specimen is positioned between the two clamps of the machine maintaining a length-to-width ratio of 4:1. The sample is deformed setting a strain rate of 10%/min of the initial length until failure. Notably, the only when the fracture is in the central zone of the specimen (i.e., far from the clamps), the test was considered valid.

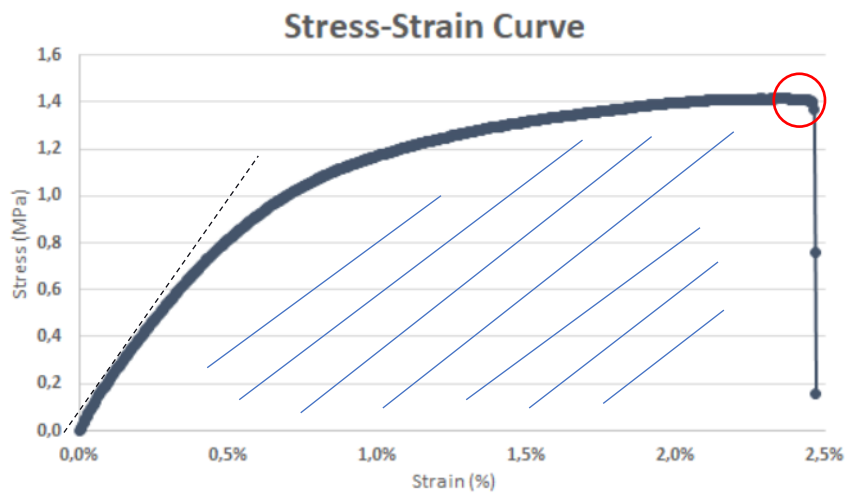


**Figure S3.** Typical keratin-based bioplastic stress-strain trend resulting during a uniaxial tensile test

Figure description:

The failure stress and strain correspond to ordinate and abscissa values at failure (red circle in figure S4). The elastic modulus is obtained from the slope of the first linear trend and the toughness correspond to area under the curve.

## 2.2. Water permeability

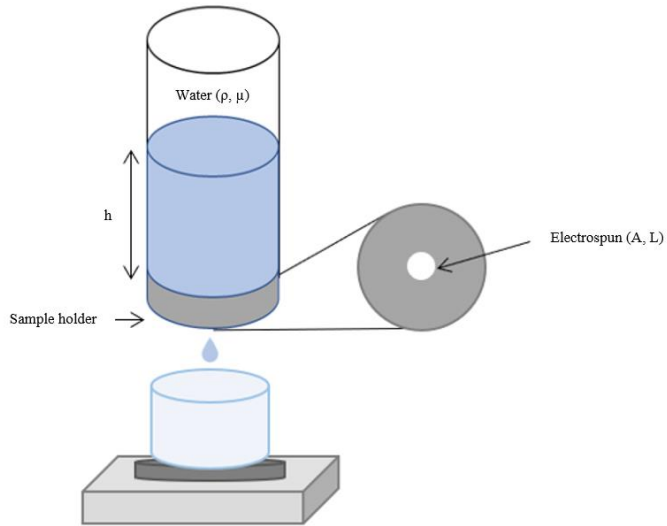


**Figure S4.** Scheme of the instrument used to evaluate the water permeability.

Figure description:

This device was composed by a vertical tube with a sample holder on its bottom. The electrospun bioplastic sample was placed into the sample holder and the vertical tube was filled with a known amount of water. This operation allowed constant pressure to be applied and driving water through the sample to calculate the permeation time.

The Darcy's law (1) was used to determine the permeability Darcy coefficient:

$$K = \frac{Q\mu L}{A\Delta P} \quad (1)$$

where, K is the Darcy coefficient [ $\text{m}^2$ ],  $\Delta P$  [Pa] is the hydrostatic pressure across the membrane,  $\mu$  is the water viscosity (0.001 Pa·s, 20°C), A is the electrospun surface [ $\text{m}^2$ ], L is the electrospun thickness [m]. The volumetric flow rate Q [ $\text{m}^3/\text{s}$ ] was calculated with the follow equation:

$$Q = \frac{\text{Slope}}{\rho} \quad (2)$$

where, the slope is derived from the curve obtained reporting the weight of the water passing through the membrane at four different timepoints (3, 5, 7, and 9 minutes) versus time, and  $\rho$  is the water density (1000 kg/m<sup>3</sup>, 20°C). Experiments were performed in triplicate.

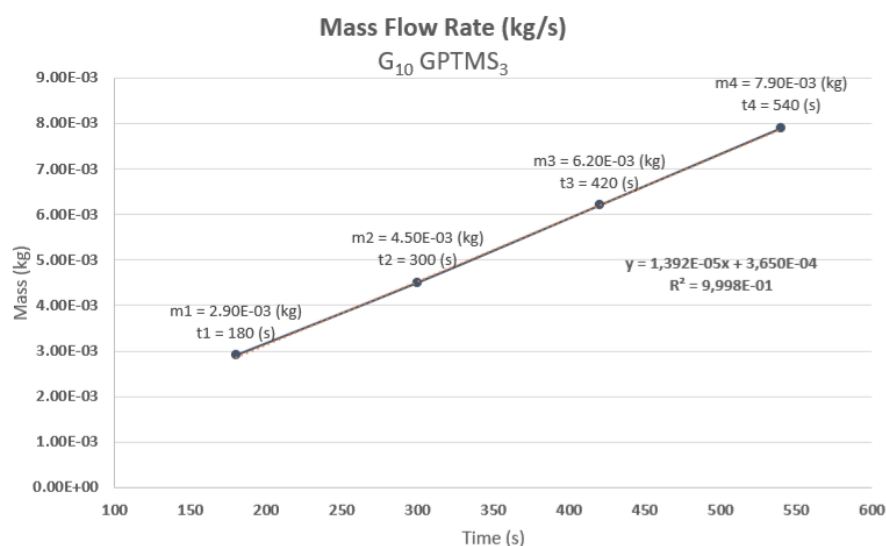
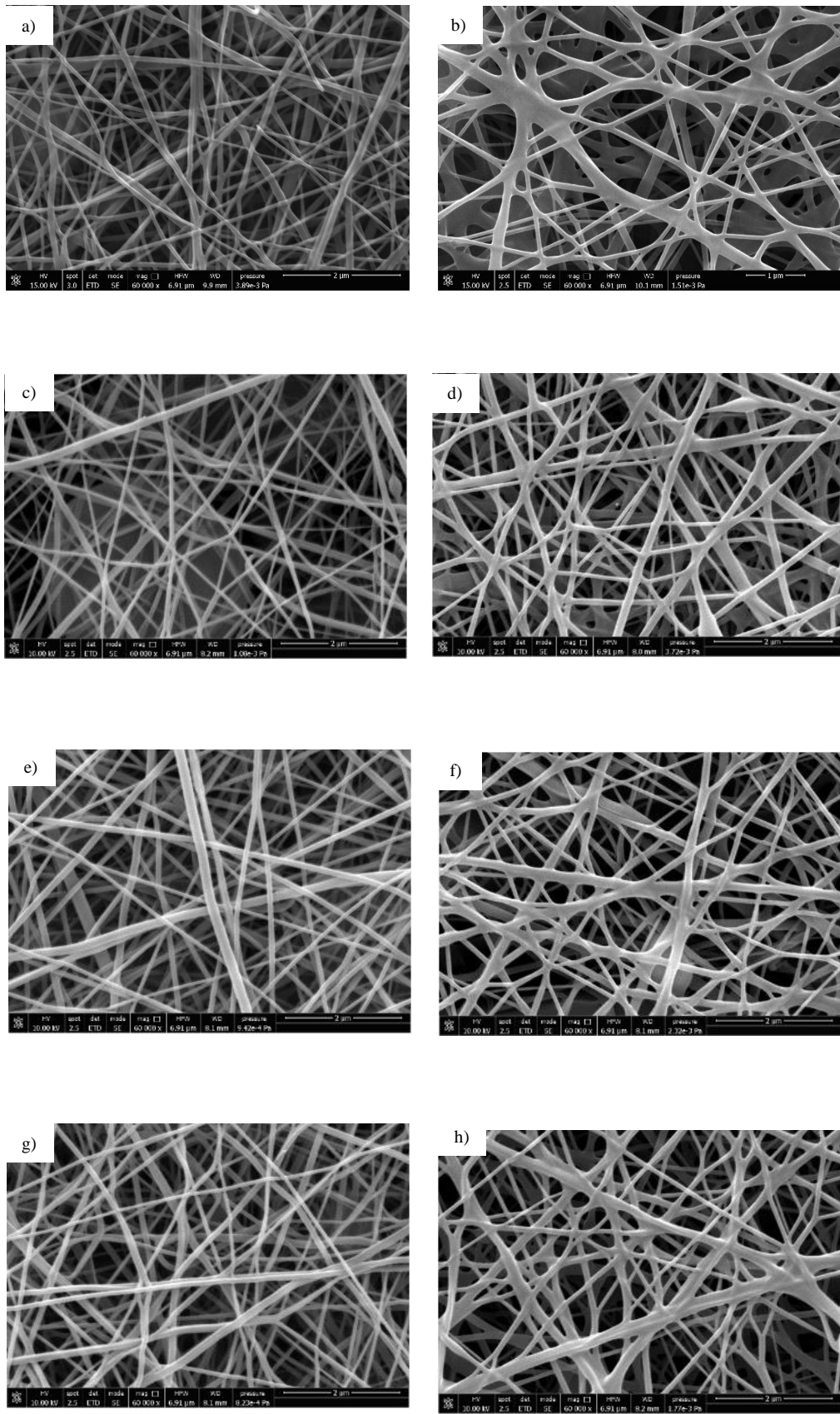


**Figure S5.** Typical curve obtained during water permeability test, weighting the water passed through the keratin-based bioplastic at 4 time point (180, 300, 420 and 540 s)

Figure description:

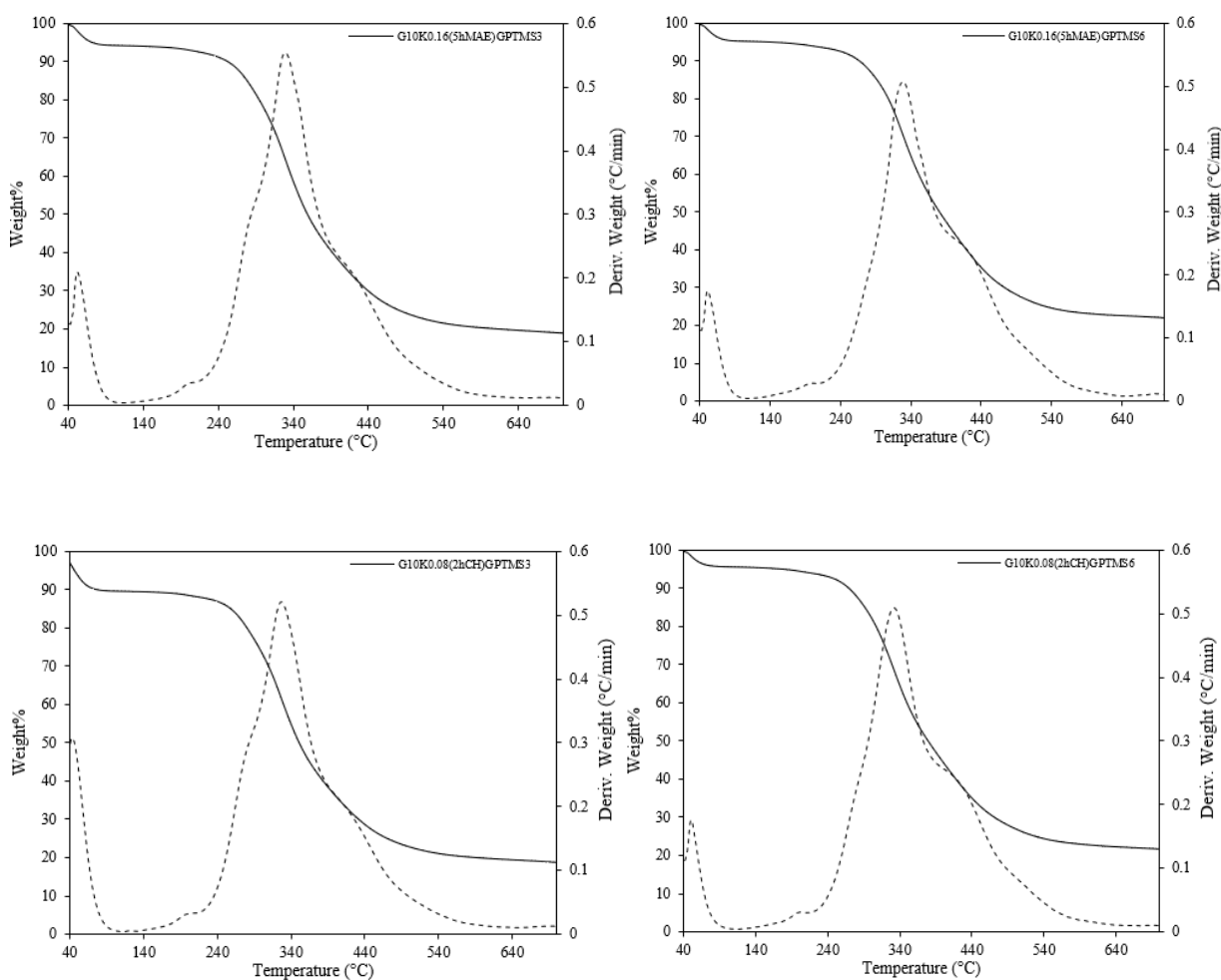
Representation of the mass flow rate  $\dot{m}$  [kg/s] evaluated as the slope of the curve obtained, during the permeability test, by collecting the weight of the water passing through the membrane at four different timepoints (3, 5, 7, and 9 minutes) versus time. Performing a linear fitting the slope is calculated and then divided by the water density to obtain the volumetric flow rate  $Q$  [m<sup>3</sup>/s] for the Darcy coefficient calculation.

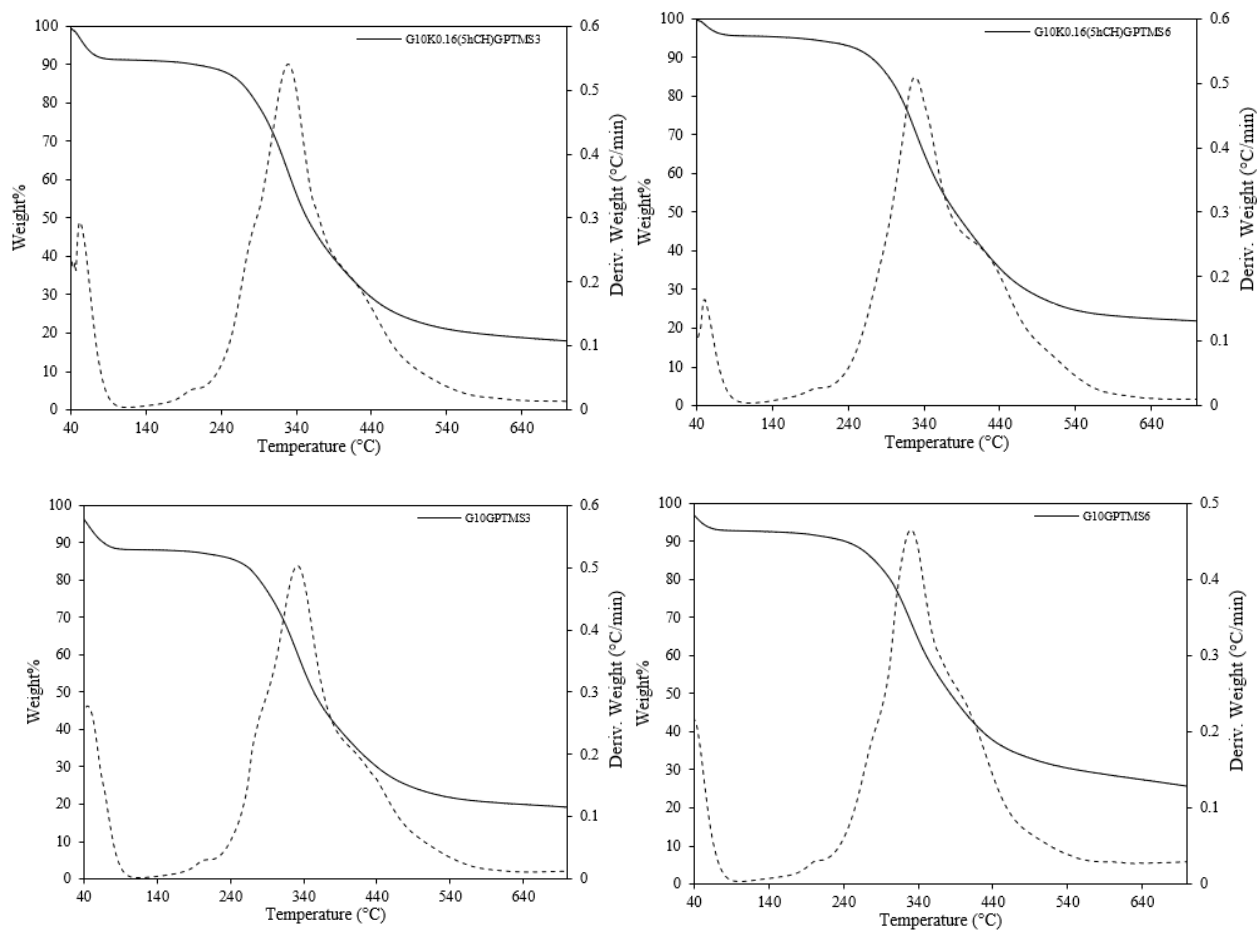
### 2.3. SEM images



**Figure S6.** SEM images of G<sub>10</sub>GPTMS<sub>3</sub> (a), G<sub>10</sub>GPTMS<sub>6</sub> (b), G<sub>10</sub>K<sub>0.08</sub>(2hCH)GPTMS<sub>3</sub> (c), G<sub>10</sub>K<sub>0.08</sub>(2hCH)GPTMS<sub>6</sub> (d), G<sub>10</sub>K<sub>0.16</sub>(5hMAE)GPTMS<sub>3</sub> (e), G<sub>10</sub>K<sub>0.16</sub>(5hMAE)GPTMS<sub>6</sub> (f), G<sub>10</sub>K<sub>0.16</sub>(5hCH)GPTMS<sub>3</sub> (g), G<sub>10</sub>K<sub>0.16</sub>(5hCH) GPTMS<sub>6</sub> (h) (magnification 60000x).

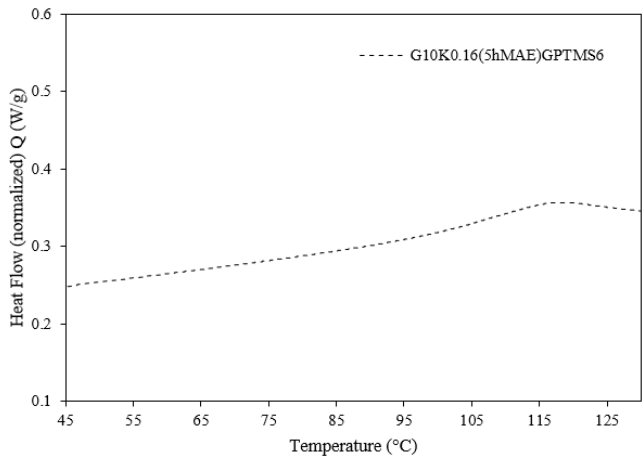
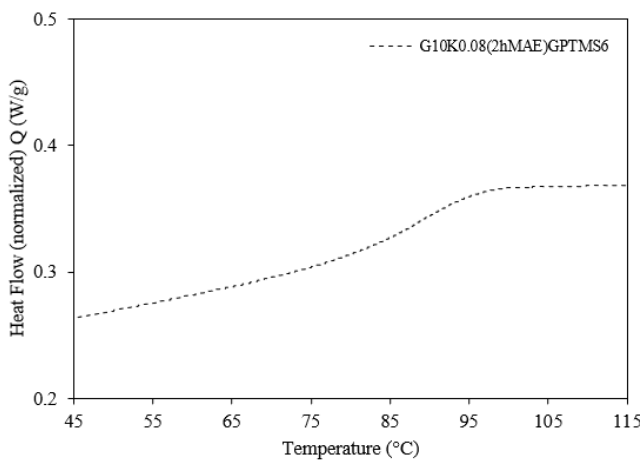
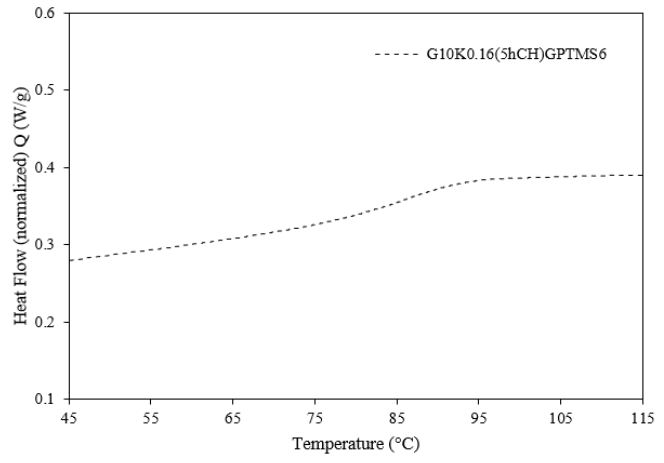
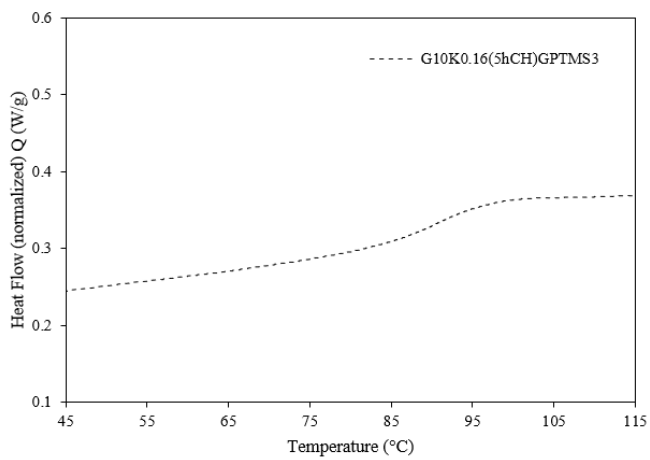
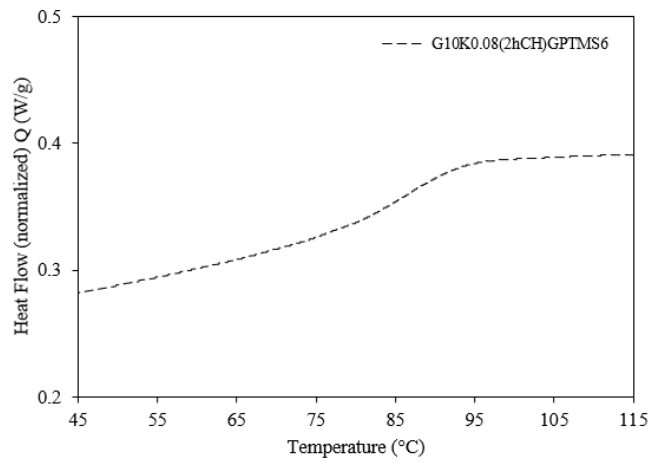
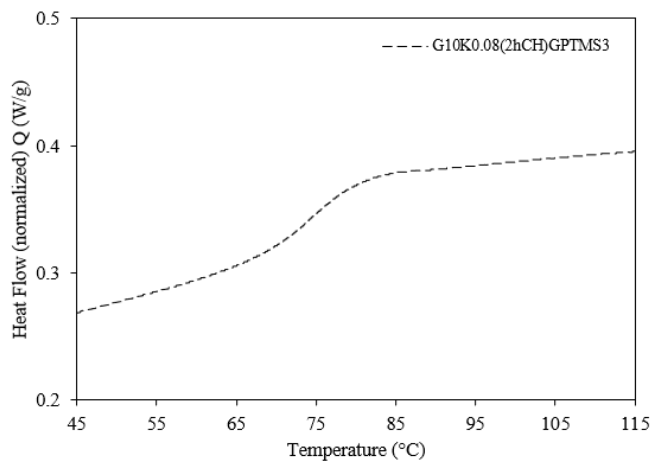
## 2.4. TG curves

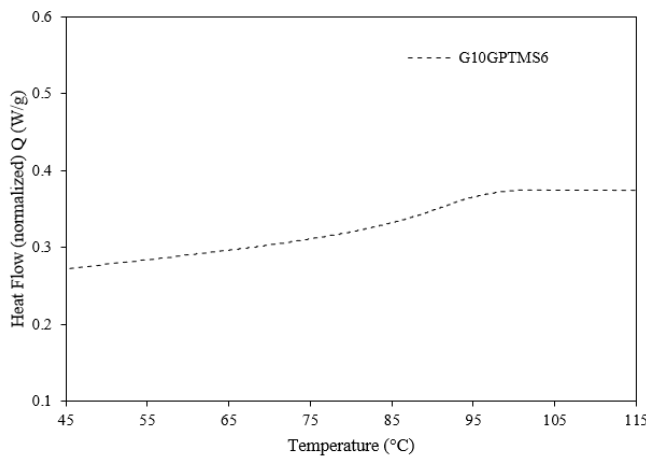




**Figure S7.** Thermogravimetric curve (solid line) and its DTG (dashed line) under nitrogen flow at  $10\text{ }^{\circ}\text{C min}^{-1}$  heating rate of  $\text{G}_{10}\text{K}_{0.16}(5\text{hMAE})\text{GPTMS}_3$ ,  $\text{G}_{10}\text{K}_{0.16}(5\text{hMAE})\text{GPTMS}_6$ ,  $\text{G}_{10}\text{K}_{0.08}(2\text{hCH})\text{GPTMS}_3$ ,  $\text{G}_{10}\text{K}_{0.08}(2\text{hCH})\text{GPTMS}_6$ ,  $\text{G}_{10}\text{K}_{0.16}(5\text{hCH})\text{GPTMS}_3$ ,  $\text{G}_{10}\text{K}_{0.16}(5\text{hCH})\text{GPTMS}_6$ ,  $\text{G}_{10}\text{GPTMS}_3$  and  $\text{G}_{10}\text{GPTMS}_6$  materials.

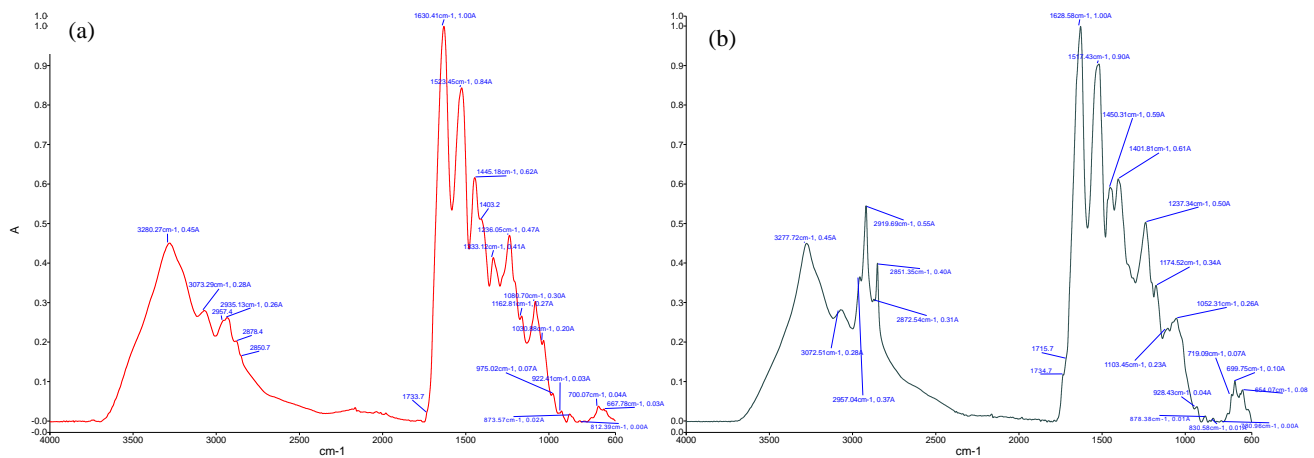
## 2.5. DSC curves

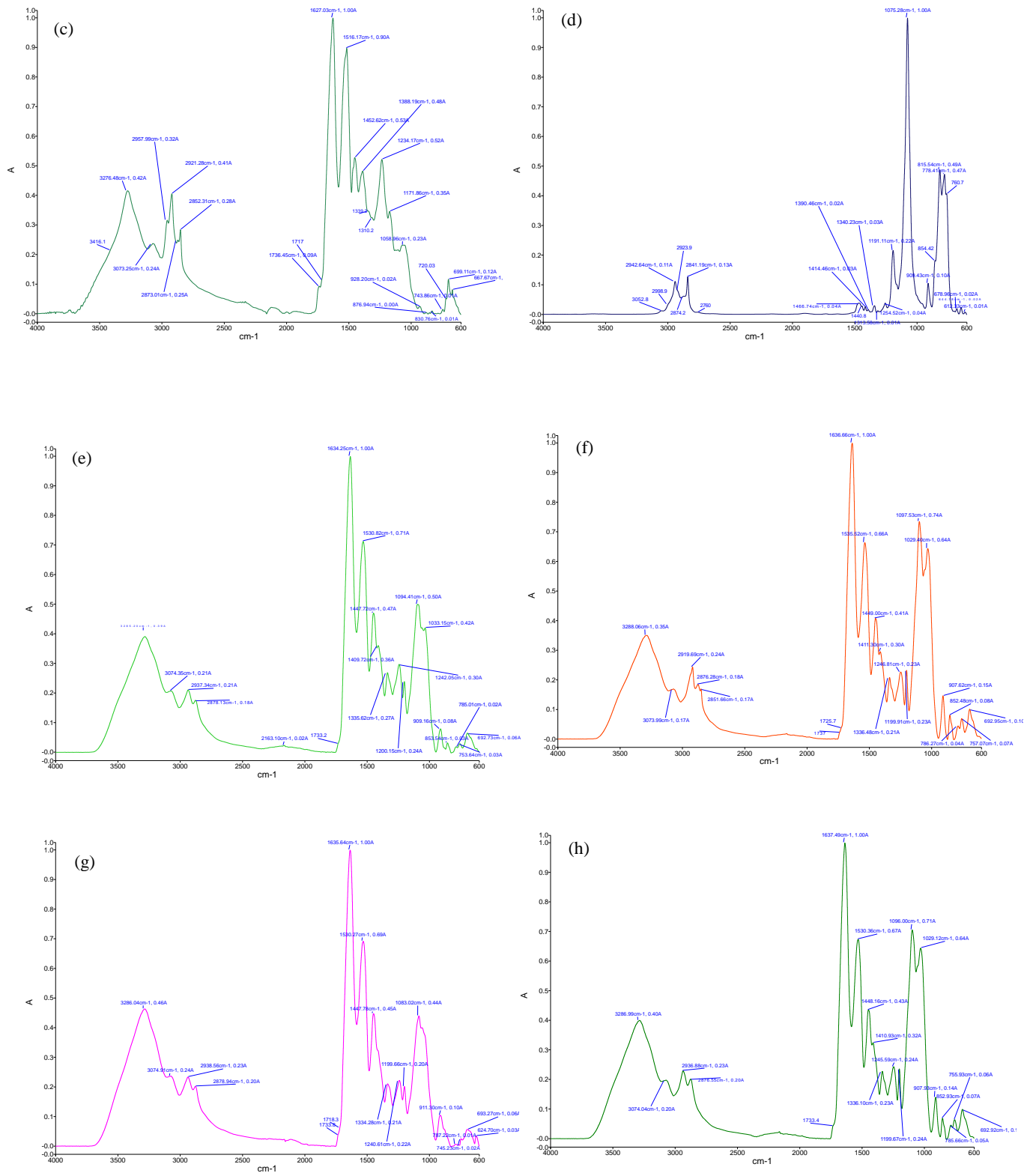




**Figure S8.** Experimental DSC curves. The heat flow normalized for sample weight obtained in the second heating scan *vs* temperature (heating rate  $10^{\circ}\text{C}\cdot\text{min}^{-1}$ ) of samples  $\text{G}_{10}\text{K}_{0.08}(2\text{hCH})\text{GPTMS}_3$ ,  $\text{G}_{10}\text{K}_{0.08}(2\text{hCH})\text{GPTMS}_6$ ,  $\text{G}_{10}\text{K}_{0.16}(5\text{hCH})\text{GPTMS}_3$ ,  $\text{G}_{10}\text{K}_{0.16}(5\text{hCH})\text{GPTMS}_6$ ,  $\text{G}_{10}\text{K}_{0.08}(2\text{hMAE})\text{GPTMS}_6$ ,  $\text{G}_{10}\text{K}_{0.08}(5\text{hMAE})\text{GPTMS}_6$ ,  $\text{G}_{10}\text{GPTMS}_6$  is reported.

## 2.6. ATR-FTIR spectra





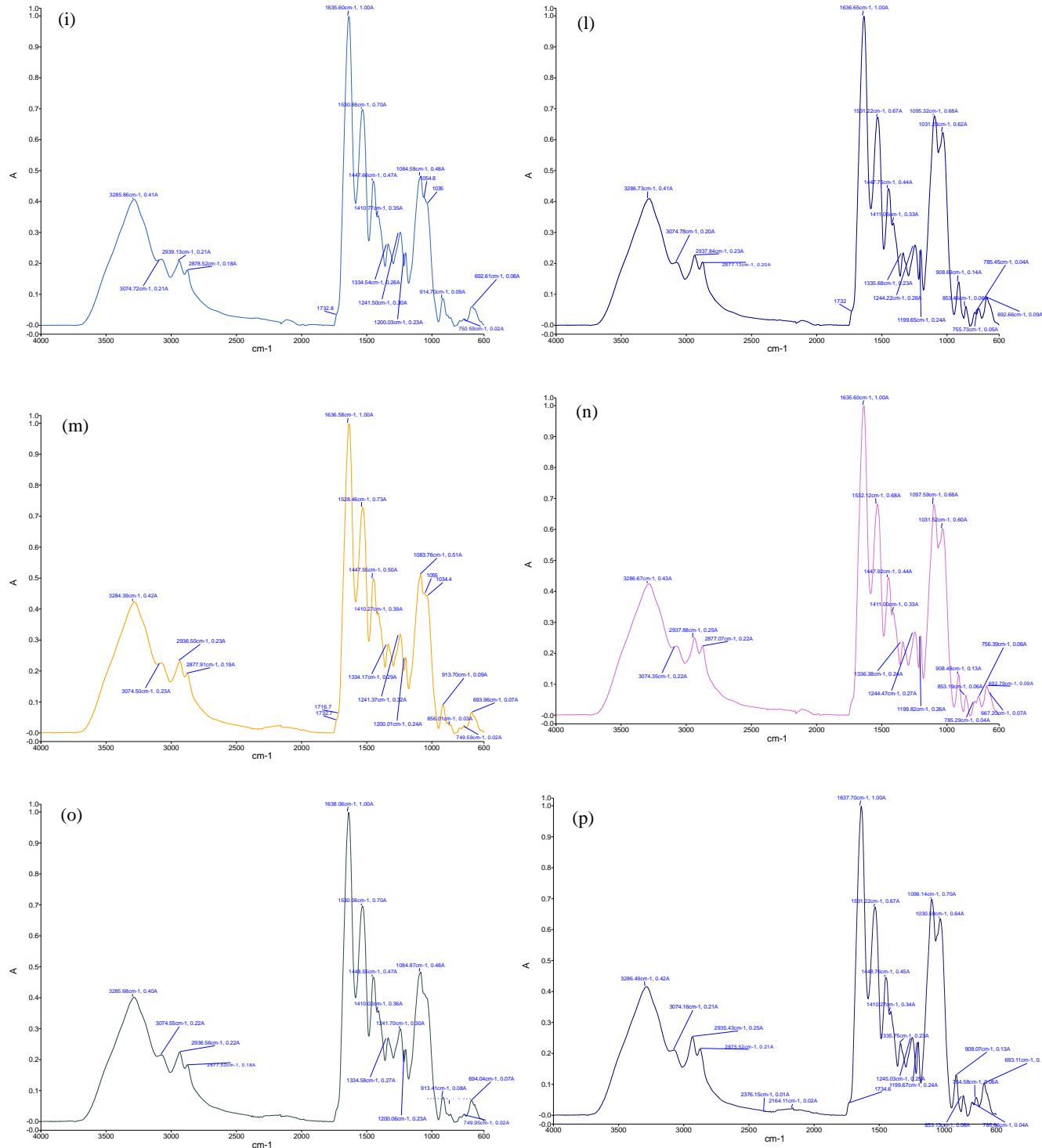


**Figure S9.** ATR-FTIR spectra of gelatine powder (a), SK<sub>IP</sub> obtained from 2h MAE extract (b)

and 5h MAE (c), GPTMS (d), G<sub>10</sub>GPTMS<sub>3</sub> (e), G<sub>10</sub>GPTMS<sub>6</sub> (f), G<sub>10</sub>K<sub>0.08</sub>(2hMAE)GPTMS<sub>3</sub> (g),

$\text{G}_{10}\text{K}_{0.08}(2\text{hMAE})\text{GPTMS}_6$  (h),  $\text{G}_{10}\text{K}_{0.16}(5\text{hMAE})\text{GPTMS}_3$  (i),  $\text{G}_{10}\text{K}_{0.16}(5\text{hMAE})\text{GPTMS}_6$  (l),  
 $\text{G}_{10}\text{K}_{0.08}(2\text{hCH})\text{GPTMS}_3$  (m),  $\text{G}_{10}\text{K}_{0.08}(2\text{hCH})\text{GPTMS}_6$  (n),  $\text{G}_{10}\text{K}_{0.16}(5\text{hCH})\text{GPTMS}_3$  (o),  
 $\text{G}_{10}\text{K}_{0.16}(5\text{hCH})\text{GPTMS}_6$  (p) materials in the 4000-600  $\text{cm}^{-1}$  regions.